Ions at the Water−Vapor Interface

M. N. Tamashiro* and M. A. Constantino

Instituto de Física "Gleb Wataghin", Universidade Estadual de Campinas, Caixa Postal 6165, 13083-970, Campinas, São Paulo, Brazil

Received: December 16, 2009; Revised Manuscript Received: January 11, 2010

We obtain the electrostatic free energy of finite-sized ions near a dielectric interface within the framework of the classical continuum dielectric theory. The ion is modeled as a dielectric sphere with a fixed uniform surface charge density. In order to avoid the generation of additional induced charges on the ionic surface, it is assumed there is no dielectric contrast between the ion core and the external dielectric medium where it is embedded, which allows an exact solution of the electrostatic problem by the image−charge method. It is shown that earlier results reported in the literature, especially when there is partial ionic penetration into the interface, always underestimate the electrostatic free energy associated with nonpolarizable ions. For an ion modeled as a vacuum cavity at the water−vapor interface, it is estimated that the free energy is an order of magnitude larger than prior predictions.

1. Introduction

A large variety of everyday phenomena of interdisciplinary interest such as capillarity, drop coalescence, fog and cloud suspension, light-particle adhesion to surfaces, the generation of static electricity by friction, the origin of atmospheric electricity, etc.,[1,2] have their properties at macro- and mesoscopic-size scales dominated by the presence of charges at interfaces. Although in many of these ordinary systems the underlying physics remains unclear, it is legitimate to treat the associated electrostatic problems by using classical continuum dielectric theory.[3−5] This theory is intrinsically macroscopic, applying the concept of linear macroscopic dielectric response to minutest distances where it may not be meaningful. Often, it assumes a sharp step-like interface, while the changes in an actual interface may occur within a width of several molecular diameters. This simplifying hypothesis should be viewed as a pragmatic approximation that can be justified only a posteriori. It ignores the discrete molecular nature of the interface, a neglect that might be questionable at the microscopic level. In spite of all this, continuum dielectric theory has been found to work well up to microscopic length scales. It has been commonly used for the description of interfacial problems at the molecular level and has been shown to be very useful in describing some aspects of real systems,[6−9] forming a basis for comparison with more accurate microscopic theories based on quantum-mechanical ab initio calculations and classical molecular-dynamics computer simulations. Despite the dramatic increase in computational power, to consider the latter in full detail may still be unfeasible for more realistic systems.

On the other hand, several fundamental phenomena in chemistry and biology are associated with electrochemical processes occurring at the interface between two immiscible fluids. Related problems include the contact potential[10] and surface tension at the liquid−liquid[11−14] and water−vapor[15−19] interfaces of electrolyte solutions, charge transfer across fluid interfaces[20,21] and membranes,[22] solvation and selective adsorption of ionic solutes at interfaces[23−31] and hydrophobic aggregates like bilayer membranes and globular proteins, bubble coalescence,[32] design of tunable optical filters,[33] atmospheric[34,35] and marine[36] environmental chemistry, water purification,[37] colloidal stability,[38−42] etc. It is not surprising that the study of such systems dates back to at least the beginning of the last century and has been attracting a lot of attention lately. In particular, Heydweiller[43] observed experimentally the increase of the water surface tension with addition of inorganic electrolytes. Wagner,[44] Onsager, and Samaras[45] (WOS) explained this effect as being caused by the ionic depletion at the water−vapor interface due to the electrostatic repulsion originated by image−charge interactions. The theory is valid in the diluted regime but exhibits strong deviations from experiments at higher concentrations.

However, recent experiments and molecular-dynamics simulations[46−50] have shown that larger halides may indeed cross and even adsorb to the water−vapor interface, contradicting, thus, the classical WOS predictions.[44,45] This phenomenon was already explored by Frumkin[51] many decades ago, who pointed out a dependence of the surface tension of electrolyte solutions on the ionic radii, but it remained a persistent controversial issue the whole time. A model for polarizable ions recently introduced by Levin[18,19] asserts that the differences in ionic size and polarizability play a prominent role in determining their properties at water−vapor interfaces. The Hofmeister specific ion effects,[52−57] well-known in biological sciences and a mystery for more than 100 years, might be rationalized by properly taking these aspects into account.

In this context, a few years ago, Kharkats and Ulstrup[58,59] (KU) obtained the electrostatic free energy of a simple model applicable to finite-sized ions near a planar interface between two homogeneous dielectric media. This model represents an adaptation of the classical Born model of ionic solvation[60] in the presence of a sharp dielectric boundary, in which the perfectly polarizable conducting sphere of the classical model[60] is replaced by a dielectric one. Their results have been quoted in reviews[61,62] and used in several works to analyze and fit experimental data[63−66] as well as in molecular-dynamics simulations[67,68] and theoretical discussions.[69,70]

In their original papers,[58,59] KU model an ion as a spherical charge distribution inside a cavity. However, they do not specify

* Corresponding author. E-mail: mtamash@ifi.unicamp.br.

10.1021/jp911898t
Published on Web 02/18/2010

the dielectric constant inside this cavity. Although far from the dielectric interface the ion-core type does not indeed matter, this is not true in the vicinity of the dielectric discontinuity. However, all of the expressions used by them correspond to those for a cavity of the same dielectric constant as the bulk medium. Curiously, their finding for a supposedly hard nonpolarizable ion sitting at the interface leads exactly to the same result derived by Levin for a perfectly polarizable ion.[18,19] Clearly, this is impossible, since a perfectly polarizable ion can rearrange its surface charge to remain hydrated, while, for a nonpolarizable ion, half of the fixed surface charge is exposed to the low-dielectric environment. Therefore, the latter case of nonpolarizable ions must necessarily be associated with higher free energies. Motivated thus by this puzzling agreement, we have decided to go through their calculations to check the plausibility of this coincidence.

The remainder of this paper is organized as follows: In section 2, we describe the model in detail, obtain the point-charge free energy in the absence of penetration by using a simple argument, and present KU results.[58,59] In section 3, we obtain the electrostatic free energy following KU's approach, pointing out their omission of the ion-core contribution to the free energy and the improper account of the image charges in the presence of penetration. In section 4, we display the free-energy profiles and compare them to KU's results, showing the increased differences for ion cores of low dielectric constant. Some concluding remarks are presented in section 5. In the two supplementary appendices, we present details of the calculations: Appendix A accounts for the electrostatic potential obtained by the image−charge method, and in Appendix B, the point-charge free energy in the absence of penetration is obtained by two alternative derivations.

2. Definition of the Model

The classical dielectric theory treats the solvent as a structureless and homogeneous dielectric continuum characterized solely by its static macroscopic bulk dielectric constant ε. The solute ions can be modeled in various ways, according to their decreased polarizability: (i) a charged conducting sphere,[19,60,71] applicable to highly polarizable ions; (ii) a fixed charge distribution embedded in a dielectric cavity or in the dielectric medium itself,[38,72,73] corresponding to semipolarizable ions; (iii) a fixed charge distribution in a vacuum cavity embedded in the dielectric, associated with nonpolarizable ions. If the ionic charge distribution is assumed to be spherically symmetric, all models are equivalent in an isotropic and homogeneous bulk medium. However, this equivalence does not hold for an inhomogeneous system consisting of two homogeneous subsystems separated by a sharp interface.

For concreteness, in order to consider a semipolarizable ion, we model it according to case ii of the preceding paragraph, as a fixed surface-charged dielectric sphere. As shown in Figure 1, we consider a spherical ion of radius a, whose center is located at $\mathbf{R} = h\hat{\mathbf{z}}$, carrying a total charge q uniformly distributed onto its *surface*, $\rho(\mathbf{r}) = \sigma\delta(|\mathbf{r}| - a)$, with $\sigma = q/4\pi a^2$ and $\mathbf{r} \equiv \mathbf{R} - h\hat{\mathbf{z}}$, whose core has the *same* dielectric constant as the medium where it is embedded. Although this might not seem a reasonable approximation, particularly when the ion penetrates the interface, it avoids the generation of additional induced charges on the ionic spherical surface,[6,74−78] simplifying the analysis of the electrostatic problem. This assumption was implicitly used in refs 58 and 59; otherwise, additional image charges due to the spherical dielectric interface should be taken into account.[6,74−78] In fact, a different dielectric constant of the ion core has already been considered for a uniform surface charge density[38] and for a general charge distribution,[72,73] but requires a nontrivial analysis and does not provide closed expressions for the free energy. Since the presence of the dielectric inside the ion partially screens the electric field, our approach provides a *lower bound* for the electrostatic free energy of an ion modeled as a vacuum cavity. The ion is in the vicinity of a planar interface, considered a boundary between two semi-infinite homogeneous media (I and II), characterized by their static dielectric constants ε_1 and ε_2. The sharp dielectric interface, located at $Z = 0$, represents the average location[79,80] of the Gibbs dividing surface (GDS). Even if the ionic center is located in region I, a distance $h > 0$ apart from the interface, one has to consider two distinct cases. In the first case (Figure 1a, $h \geq a$), the ion is completely immersed in region I, while in the second case (Figure 1b, $a > h > 0$) the ion is partially penetrating into region II, but its center is still located in region I.

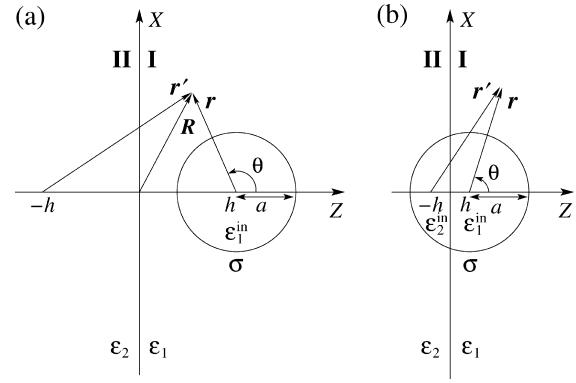

Figure 1. Two-dimensional representation (cross section at the $Y = 0$ plane) of spherical ion of radius a, charge q, and uniform fixed surface-charge density $\sigma = q/4\pi a^2$. The ionic center is located in region I, at $\mathbf{R} = h\hat{\mathbf{z}}$, a distance $h > 0$ apart from a planar interface at $Z = 0$ between two semi-infinite homogeneous media of static dielectric constants ε_1 and ε_2. The internal dielectric constants $\varepsilon_k^{\text{in}}$ are taken the same as of the external medium where the ion is embedded $\varepsilon_k^{\text{in}} = \varepsilon_k$. Case a: $h \geq a$, the ion is completely embedded in region I. Case b: $a > h > 0$, the ion partially penetrated into region II.

As stated in the last paragraph, the internal dielectric constant of the spherical ion is considered to be the same as of the external medium where it is embedded. In the absence of ionic penetration into the interface—Figure 1a, $h \geq a$—it is straightforward to solve the electrostatic problem by the image−charge method.[81−83] For mathematical convenience, we introduce the dimensionless parameter

$$\lambda \equiv \frac{\varepsilon_1 - \varepsilon_2}{\varepsilon_1 + \varepsilon_2} \tag{1}$$

which measures the dielectric contrast across the planar interface between the two semi-infinite homogeneous media. Taking into account that there is no *free* charge in region II nor along the planar interface, the problem reduces to the evaluation of the interaction energy of two nonoverlapping spherical shells of radius a, carrying fixed surface charge densities σ and $\lambda\sigma$, whose centers are located at $h\hat{\mathbf{z}}$ and $-h\hat{\mathbf{z}}$, respectively, immersed in an infinite medium of dielectric constant ε_1. By Gauss' law, the two spherically symmetric distributions may be replaced by point charges q and λq located at the respective sphere centers. Therefore, to obtain the electrostatic free energy W, one needs to add to the ionic self-energy in bulk medium I,[84]

$W_1^{self} = q^2/2\varepsilon_1 a$, the ion−image interaction of the point charges q and λq a distance of $2h$ apart

$$W(x \geq 1) = \frac{q^2}{2\varepsilon_1 a}\left(1 + \frac{\lambda}{2x}\right) \tag{2}$$

with $x \equiv h/a$. The additional $^1/_2$ factor comes from the Güntelberg charging process.[85−87] This is the classical point-charge result[5] and the ion−image contribution due to the presence of the interface, proportional to λ, does not depend, indeed, on the ionic radius a.

Using the same arguments which led to eq 2, if the spherical ion—now with internal dielectric constant ε_2—is completely immersed in region II, $h \leq -a$, one obtains

$$W(x \leq -1) = \frac{q^2}{2\varepsilon_2 a}\left(1 - \frac{\lambda}{2|x|}\right) = \frac{q^2}{2\varepsilon_1 a}\left(\frac{1+\lambda}{1-\lambda}\right)\left(1 + \frac{\lambda}{2x}\right) \tag{3}$$

Surprisingly, our expressions for the electrostatic free energy in the absence of penetration, eqs 2 and 3, differ from KU's prior reported results.[58,59] In view that their original works, as well as subsequent papers that cite them, contain some misprints, we also give explicitly their predictions in dimensionless form, $w_{KU} \equiv W_{KU}/W_1^{self}$, including the case with penetration depicted in Figure 1b for $|h| < a$, to be considered by us later in section 3

$$w_{KU}(x \geq 1) = 1 + \frac{\lambda}{2x} + \frac{\lambda^2}{2}\left[\frac{1}{4x}\ln\left(\frac{2x+1}{2x-1}\right) + \frac{1}{1-(2x)^2}\right] \tag{4}$$

$$w_{KU}(0 < x < 1) = 1 + \lambda\left(1 - \frac{x}{2}\right) + \frac{\lambda^2}{4}\left[\frac{1}{2x}\ln(1+2x) + \frac{1}{1+2x} + x - 2\right] \tag{5}$$

$$w_{KU}(x = 0) = 1 + \lambda \tag{6}$$

$$w_{KU}(-1 < x < 0) = \left(\frac{1+\lambda}{1-\lambda}\right)\left\{1 - \lambda\left(1 + \frac{x}{2}\right) - \frac{\lambda^2}{4}\left[\frac{1}{2x}\ln(1-2x) - \frac{1}{1-2x} + x + 2\right]\right\} \tag{7}$$

$$w_{KU}(x \leq -1) = \left(\frac{1+\lambda}{1-\lambda}\right)\left\{1 + \frac{\lambda}{2x} + \frac{\lambda^2}{2}\left[\frac{1}{4x}\ln\left(\frac{2x+1}{2x-1}\right) + \frac{1}{1-(2x)^2}\right]\right\} \tag{8}$$

Comparing the simple and exact point-charge results, eqs 2 and 3, with the analogue eqs 4 and 8 found by KU,[58,59] there is clearly a disagreement, represented by the last additional terms proportional to λ^2. Therefore, in order to find the source of the discrepancy, it is necessary to trace back and comment on their calculations.

3. Electrostatic Free Energy

The electrostatic free energy associated with a *free* charge density $\rho(\mathbf{r})$ distributed over the volume V may be obtained by[83]

$$W = \frac{1}{2}\int_V \rho(\mathbf{r})\Psi(\mathbf{r})\, d^3\mathbf{r} \tag{9}$$

The *total* electrostatic potential $\Psi(\mathbf{r})$ includes contributions generated by free and induced charges. On the other hand, the induced charges should not be included in the *free* charge distribution $\rho(\mathbf{r})$. Equation 9 is valid in a vacuum as well as in a linear dielectric, for which it holds the linear dielectric response $\mathbf{D} = \varepsilon\mathbf{E}$, where $\mathbf{D}$ and $\mathbf{E} = -\nabla\Psi$ are the displacement and electrostatic fields. Using standard vector algebra,[83] eq 9 may be transformed into equivalent forms

$$\begin{aligned} W &= \frac{1}{8\pi}\int_V \varepsilon(\mathbf{r})|\nabla\Psi|^2\, d^3\mathbf{r} - \frac{1}{8\pi}\int_V \nabla\cdot[\varepsilon(\mathbf{r})\Psi\nabla\Psi]\, d^3\mathbf{r} \\ &= \frac{1}{8\pi}\int_V \varepsilon(\mathbf{r})|\mathbf{E}|^2\, d^3\mathbf{r} - \frac{1}{8\pi}\int_{\partial V} \varepsilon(\mathbf{r})\Psi\nabla\Psi\cdot d\mathbf{S} \end{aligned} \tag{10}$$

In eq 10, the volume of integration V must include all regions where the free-charge distribution $\rho(\mathbf{r})$ does not vanish and ∂V represents the closed surface that delimits V. By choosing different forms to obtain W, it is then possible to check any inconsistency of the calculations. In particular, for the problem in consideration, if one takes an infinite volume, the surface contribution vanishes, whereas for an infinitesimal volume around the ionic charged surface at $r = a$, only the surface terms contribute. The route taken by KU[58,59] to obtain the free energy corresponds to the latter choice, leading to eqs 4−8. However, as will be shown below, there are some omissions and misinterpretations in their procedure.

In order to evaluate the integrals given by eqs 9 and 10, it is necessary to obtain the total electrostatic potential Ψ of the system. Using the image−charge method,[81−83] it is possible to exactly solve the electrostatic problem, whose details are given in Appendix A.

3.1. Case without Penetration, $|h| \geq a$. As commented in section 2, the point-charge free energy, eq 2, may be directly obtained from the point-charge ion−image interaction and the Güntelberg charging process. This simple result disagrees with the calculations of KU,[58,59] who obtained a different expression, eq 4, for the electrostatic free energy in the simpler case $x \geq 1$ in the absence of penetration. We show next that an accurate evaluation of eq 10 leads indeed to the point-charge free energy, eq 2, as expected.

Let us evaluate eq 10 by taking an infinitesimal volume around the ionic charged surface at $r = a$. The first (volumetric) term vanishes, since the thickness of the ionic charged shell is infinitesimal and there is no divergence of the electrostatic field $\mathbf{E}$ at $r = a$. The electrostatic free energy may be split into two surface contributions

$$\begin{aligned} W_> &\equiv \frac{\varepsilon_1}{8\pi}\int_{S_{1>}} \Psi_{1>}\nabla\Psi_{1>}\cdot d\mathbf{S}_{1>} \\ &= \frac{q^2}{2\varepsilon_1 a}\left\{1 + \frac{\lambda}{2x} + \frac{\lambda^2}{2}\left[\frac{1}{4x}\ln\left(\frac{2x+1}{2x-1}\right) + \frac{1}{1-(2x)^2}\right]\right\} \end{aligned} \tag{11}$$

$$\begin{aligned} W_< &\equiv \frac{\varepsilon_1}{8\pi}\int_{S_{1<}} \Psi_{1<}\nabla\Psi_{1<}\cdot d\mathbf{S}_{1<} \\ &= -\frac{\lambda^2 q^2}{4\varepsilon_1 a}\left[\frac{1}{4x}\ln\left(\frac{2x+1}{2x-1}\right) + \frac{1}{1-(2x)^2}\right] \end{aligned} \tag{12}$$

associated, respectively, with the external and internal surfaces $S_{1>}$ and $S_{1<}$ that delimit the volumes outside ($Z > 0$, $r > a$) and

TABLE 1: Dimensionless Free Energies upon Contact $W(x = \pm 1)/W_1^{self}$ for Conducting-Sphere (cs),[19,71] Point-Charge/Mixed-Dielectric (md), eqs 2 and 3, and Vacuum-Cavity (vc) Models[a]

$x = 1$	(side of higher dielectric constant)		
$(\varepsilon_1, \varepsilon_2)$	cs	md	vc
(78, 1)	1.4325	1.487	1.547
(78, 2)	1.4225	1.475	1.531
$x = -1$	(side of lower dielectric constant)		
$(\varepsilon_1, \varepsilon_2)$	cs	md	vc
(78, 1)	20.68	39.987	39.987
(78, 2)	12.368	20.475	21.046

[a] The vacuum-cavity results are obtained by using the approximate expressions of the dielectric-sphere model[72,73] with $\varepsilon^{in} = 1$. These estimates are consistent with numerical values of the exact solution reported for a restricted set of parameters.[38] The different cases are labeled by the higher and lower dielectric constants $(\varepsilon_1, \varepsilon_2)$.

inside ($Z > 0$, $r < a$) the ion in region I. To integrate eqs 11 and 12, we use the electrostatic potentials given by eqs A.1 and A.2 in Appendix A. Notice the sign inversion between eq 10, and eqs 11 and 12, since the normal vector of the original surface of integration ∂V points outward the spherical shell at $r = a$. As expected, the final result for the electrostatic free energy, $W = W_> + W_<$, coincides with the point-charge result, eq 2.

KU[58,59] obtained the electrostatic free energy for $x \geq 1$, eq 4, by considering solely the contribution due to the external surface, eq 11, $W_{KU} = W_>$. The contribution $W_<$ due to the internal surface, eq 12, was neglected in refs 47 and 48 by the incorrect argument that the electric field **E** vanishes in the ion core—see eq A.1 of Appendix A. Therefore, the additional term obtained by KU[58,59] in eq 4, proportional to λ^2, is due to the omission of $W_<$. Once the internal contribution is properly included, $W = W_> + W_<$, this spurious correction cancels out and one regains the point-charge electrostatic free energy, eq 2. Outside the penetration region, however, $W_<$ is small, so that the KU result does not differ much from the correct expression given by eq 2—see section 4 and Figure 4.

In Appendix B, it is shown that eq 2 may also be obtained either by directly integrating eq 9 or by eq 10 applied to an infinite volume. Both forms lead to the point-charge expression, eq 2, in disagreement with KU results.[58,59] In all cases, one can trace back the discrepancies to their neglect of the contribution $W_<$ of the ionic core to the electrostatic free energy, eq 12. However, this contribution cannot be disregarded, and the correct result should indeed correspond to the point-charge electrostatic free energy, eq 2.

In the absence of penetration, there are reported exact results for conducting spheres[19,71] and approximate expressions for a monopole inside a spherical dielectric cavity.[72,73] These allow a comparison between the different treatments of the internal ionic region. In Table 1, we present the dimensionless free energies upon contact $w(x = \pm 1) \equiv W(x = \pm 1)/W_1^{self}$ for the distinct models. The contact cases provide the largest deviations without penetration. One can see that the relative deviations are small—they differ no more than 5%—as already pointed out by Levin.[19] Therefore, unless the ion center is very close to the interface, the finite-sized and image−charge effects are small. Moreover, one notices that the lower the dielectric constant of the ion core, the higher the associated free energy. The limit of conducting spheres may be taken as $\varepsilon^{in} \to \infty$.

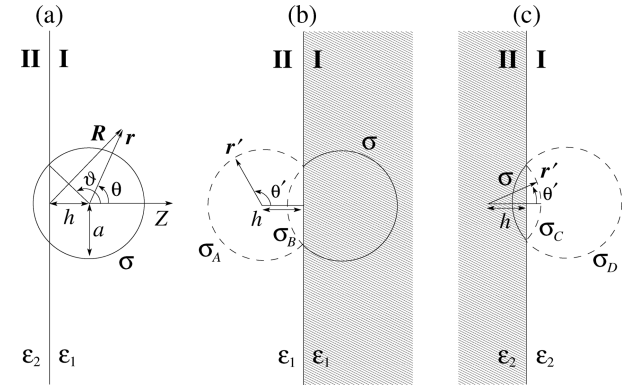

Figure 2. Two-dimensional representation (cross section at the $Y = 0$ plane) of a spherical ion of radius a, whose center is located at $\mathbf{R} = h\hat{\mathbf{z}}$ in region I of dielectric constant ε_1. The ion is partially penetrating into region II ($0 < h < a$). The shaded regions represent the semi-infinite space where the electrostatic potential is being calculated and the solid and dashed lines correspond to the configurations of real and image charges, respectively. (a) Real configuration of charges; (b) equivalent configuration of real and image charges for the calculation of the potential in region I, with $\sigma_A = \lambda\sigma$ and $\sigma_B = (1 + \lambda)\sigma$; (c) equivalent configuration of real and image charges for the calculation of the potential in region II, with $\sigma_C = -\lambda\sigma$ and $\sigma_D = (1 - \lambda)\sigma$.

3.2. Case with Penetration, $|h| < a$. In order to solve the electrostatic problem when the ion partially penetrates the interface ($a > h > 0$), as shown in Figure 1b, KU[58,59] proceed with the calculations by using eqs A.1−A.3, but these simple expressions no longer apply to this case. There are free charges on both sides of the dielectric interface, and one needs to take them properly into account to compute the electrostatic potential, as shown in Figure 2. Therefore, one cannot replace the induced charges by a simple point-like image charge, as given by eqs A.1−A.3. In this case, the image charges are associated with sections of spherical shells and it is not possible to obtain analytical closed forms for the electrostatic potential and free energy. One needs, therefore, to resort to numerical calculations to obtain the electrostatic free energy W.

Let us pose the electrostatic problem in terms of image charges, as sketched in Figure 2. The image−charge method[81−83] may still be applied for each infinitesimal surface charge element on the ionic surface, giving rise to an image−charge surface distribution obtained either by mirror reflection about the planar interface at $Z = 0$ or by applying an image factor of $\pm\lambda$ and keeping the charge element at the original position. However, as shown in Figure 2, the whole image−charge distribution is no longer spherically symmetric. The electrostatic potential in region I is equivalent to that generated by a spherical shell with uniform surface charge density σ centered at $\mathbf{R} = h\hat{\mathbf{z}}$ and two sections of spherical shells with uniform surface charge densities $\sigma_A = \lambda\sigma$ and $\sigma_B - \sigma = \lambda\sigma$ centered at $\mathbf{R} = \mp h\hat{\mathbf{z}}$, all embedded in an infinite dielectric medium of constant ε_1. On the other hand, the electrostatic potential in region II is equivalent to that generated by a spherical shell with uniform surface charge density σ centered at $\mathbf{R} = h\hat{\mathbf{z}}$ and two sections of spherical shells with uniform surface charge densities $\sigma_C = -\lambda\sigma$ and $\sigma_D - \sigma = -\lambda\sigma$ centered at $\mathbf{R} = \mp h\hat{\mathbf{z}}$, all embedded in an infinite dielectric medium of constant ε_2. The electrostatic potentials Ψ_k generated by these effective charge distributions, evaluated at the ionic surface $r = a$, are given by eqs A.11 and A.12 in Appendix A. Replacing them into the simpler form eq 9, one obtains the electrostatic free energy associated with each semi-infinite region

$$W_1 = \frac{1}{2}\int_{r=a} \sigma\Psi_1(r, 0 \le \theta \le \vartheta)\, \mathrm{d}S_1 = \frac{q^2}{4\varepsilon_1 a}\{1 + x + \lambda[I_A(x) + I_B(x)]\} \quad (13)$$

$$W_2 = \frac{1}{2}\int_{r=a} \sigma\Psi_2(r, \vartheta \le \theta \le \pi)\, \mathrm{d}S_2 = \frac{q^2}{4\varepsilon_2 a}\{1 - x - \lambda[I_A(-x) + I_B(-x)]\} \quad (14)$$

with $\mathrm{d}S_k = a^2\mathrm{d}\phi\mathrm{d}(\cos\theta)$, $\vartheta = \arccos(-x)$—see Figure 2—and we introduce the two-dimensional integrals

$$I_A(x) \equiv \frac{1}{\pi\sqrt{2}}\int_{-x}^{1} \mathrm{d}(\cos\theta)\int_{-1}^{x} \mathrm{d}(\cos\theta')\times \frac{K\left[\frac{2\sin\theta\sin\theta'}{1-\cos(\theta+\theta')+2x(\cos\theta-\cos\theta'+x)}\right]}{\sqrt{1-\cos(\theta+\theta')+2x(\cos\theta-\cos\theta'+x)}} \quad (15)$$

$$I_B(x) \equiv \frac{1}{\pi\sqrt{2}}\int_{-x}^{1} \mathrm{d}(\cos\theta)\int_{x}^{1} \mathrm{d}(\cos\theta')\frac{K\left[\frac{2\sin\theta\sin\theta'}{1+\cos(\theta-\theta')}\right]}{\sqrt{1+\cos(\theta-\theta')}} = \frac{2}{\pi}\int_0^{(1+x)/(1-x)} \frac{\mathrm{d}u}{(1+u)^{3/2}}\int_0^{(1-x)/(1+x)} \frac{\mathrm{d}v}{(1+v)^{3/2}}K[uv] \quad (16)$$

in terms of the complete elliptic integral of the first kind,[88,89]

$$K[m] \equiv \int_0^{\pi/2} \frac{\mathrm{d}\alpha}{\sqrt{1 - m\sin^2\alpha}} \quad (17)$$

The total electrostatic free energy $W = W_1 + W_2$ reads

$$W(|x|<1) = \frac{q^2}{2\varepsilon_1 a}\left(\frac{1}{1-\lambda}\right)\left\{1 - \frac{\lambda x}{2}(1-\lambda) - \lambda^2[I_A(x) + I_B(x)]\right\} \quad (18)$$

where we used the symmetry relations $I_A(x) = I_A(-x) + x$, $I_B(x) = I_B(-x)$. Some particular values of the integrals are $I_A(x = 1) = 1$, $I_A(x = -1) = I_B(x = 1) = 0$, $I_A(x = 0) = I_B(x = 0) = 0.3633802...$, but in general, one has to rely on numerical calculations to evaluate them. It should be remarked that eq 18 also holds when there is partial penetration and the ionic center is located in region II, $-1 < x < 0$. One only needs to swap the dielectric constants $\varepsilon_1 \rightleftarrows \varepsilon_2$, $\lambda \to -\lambda$, and $x \to |x| = -x$, which leaves the whole expression for W, eq 18, unchanged.

Instead of eq 18, KU obtained their analogue electrostatic free energy for $0 < x < 1$, eq 5, by $W_{KU} = \tilde{W}_1 + \tilde{W}_2$, through the evaluation of the *external* surface integrals[58,59] by using the same electrostatic potentials, eqs A.1−A.3, which are strictly valid only for the case in the absence of penetration ($x \ge 1$)

$$\tilde{W}_1 \equiv \frac{\varepsilon_1}{8\pi}\int_{S_{1>}} \Psi_{1>}\nabla\Psi_{1>}\cdot\mathrm{d}\boldsymbol{S}_{1>} = \frac{q^2}{4\varepsilon_1 a}\left\{1 + x + \lambda(2-x) + \frac{\lambda^2}{2}\left[\frac{1}{2x}\ln(1+2x) + \frac{(1+x)(1-2x)}{1+2x}\right]\right\} \quad (19)$$

$$\tilde{W}_2 \equiv \frac{\varepsilon_2}{8\pi}\int_{S_{2>}} \Psi_2\nabla\Psi_2\cdot\mathrm{d}\boldsymbol{S}_{2>} = \frac{q^2}{4\varepsilon_2 a}(1-\lambda)^2(1-x) \quad (20)$$

The above procedure to obtain W_{KU}, however, is flawed because (i) it does not take properly into account all image charges; (ii) it overlooks the contribution of the internal ionic region. There is no simple way to reconcile eqs 13 and 14, and eqs 19 and 20. Furthermore, opposed to the prior case in the absence of penetration, now the discrepancies are pronounced—see Figure 4—notably for a nonpolarizable ion associated with an internal low-dielectric constant. This deviation can be inferred, in view that, aside from the missing image charges, most of the electrostatic free energy for the ion sitting exactly at the interface concentrates in the electrostatic field inside the ion core, precisely the term that KU overlooked.[58,59]

4. Electrostatic Free-Energy Profile

Normalizing eqs 2, 3, and 18 to the ionic self-energy in the bulk region I, $W_1^{self} = q^2/2\varepsilon_1 a$, leads to the dimensionless free energy $w \equiv W/W_1^{self}$

$$w(x \ge 1) = 1 + \frac{\lambda}{2x} \quad (21)$$

$$w(|x|<1) = \left(\frac{1}{1-\lambda}\right)\left\{1 - \frac{\lambda x}{2}(1-\lambda) - \lambda^2[I_A(x) + I_B(x)]\right\} \quad (22)$$

$$w(x \le -1) = \left(\frac{1+\lambda}{1-\lambda}\right)\left(1 + \frac{\lambda}{2x}\right) \quad (23)$$

displayed in Figure 3. In the bulk region II, $w(x \ll -1) \approx (1 + \lambda)/(1 - \lambda) = \varepsilon_1/\varepsilon_2$, while in the opposite limit, in the bulk region I, $w(x \gg 1) \approx 1$. In these two asymptotic cases, far from the dielectric interface, the electrostatic free energy W reduces to the solvation energies associated with the two homogeneous bulk media, since the dielectric interface has a negligible effect. The difference between these two solvation energies is usually called the Born energy,[60] which corresponds to the energy of ion transfer between these two bulk media.

We compare eqs 21−23 with the analogue expressions obtained by KU, eqs 4−8. One can see that the λ and x dependence of the two sets of equations are quite different. In particular, outside the penetration region, $|x| \ge 1$, our results are given by the point-charge expressions. Figure 4 displays the ratio between our calculations, eqs 21−23, and the results given by KU,[58,59] eqs 4−8. Observe that the larger the dielectric contrast λ between the two media, the bigger the deviations of the two calculations—see inset of Figure 4. They become especially important inside the penetration region, $|x| < 1$. In

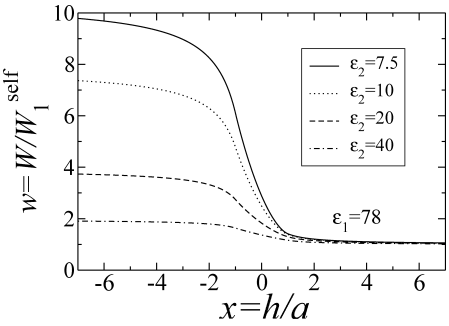

Figure 3. Dimensionless electrostatic free-energy profile $w \equiv W/W_1^{self}$ of a spherical ion of radius a, charge q, and fixed uniform surface-charge density $\sigma = q/4\pi a^2$, located a distance h apart from a planar dielectric interface between two semi-infinite media of dielectric constants ε_1 (located at $x > 0$) and ε_2 (located at $x < 0$). The numerical values were obtained for $\varepsilon_1 = 78$ (water at room temperature) and several values of ε_2 corresponding to less polar solvents.

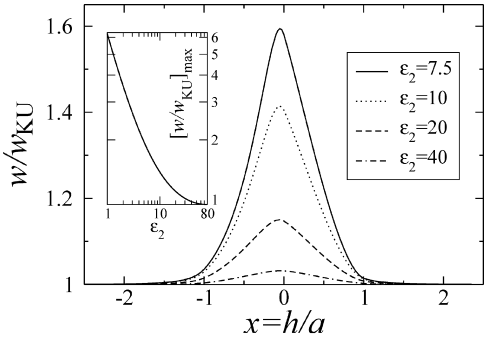

Figure 4. Ratio of the dimensionless free-energy profiles $w(x)$ given by eqs 21−23, and $w_{KU}(x)$ results,[47,48] eqs 4−8. The numerical values were obtained for $\varepsilon_1 = 78$ (water at room temperature, located at $x > 0$) and several ε_2 values associated with less polar solvents (located at $x < 0$). The inset displays the maximum of the ratio profile—located very close to the GDS, $x \approx 0$—as a function of the lower dielectric constant ε_2. As one can see, the largest deviations occur for a mixed water−vacuum cavity ($\varepsilon_2 = 1$).

particular, for a water−vapor interface, $\varepsilon_1 = 78$ and $\varepsilon_2 = 1$, the largest relative deviation is obtained for an ion sitting very close to the GDS, $x \approx -0.011$, yielding $[w/w_{KU}]_{max} \approx 6.23$, as shown in the inset of Figure 4. At the scale presented in Figure 4, the largest deviation is indistinguishable from the value calculated exactly at the GDS, $w(x = 0)/w_{KU}(x = 0) \approx 6.19$. Recalling that KU obtained $w_{KU}(x = 0) = 1 + \lambda$—which incidentally is identical to the exact result for a conducting sphere[18,19]—we have $W_{KU}(x = 0) = W_{cs}(x = 0) \approx 1.97W_1^{self}$, while, for the mixed-dielectric model, we have $W_{md}(x = 0) \approx 12.22W_1^{self}$.

Since the presence of an internal dielectric lowers the ionic self-energy, if we have a complete vacuum cavity ($\varepsilon_1^{in} = \varepsilon_2^{in} = 1$), one expects that the associated electrostatic free energy becomes even higher. A rough estimate is a factor of 2 for the free-energy ratio of an ion modeled as a vacuum cavity compared to a mixed dielectric. Therefore, KU calculations[58,59] underestimate the electrostatic free energy of a nonpolarizable ion near the GDS by more than an order of magnitude! For a hard nonpolarizable ion (vacuum cavity), Levin's theory[19] predicts $W_{vc}(x = 0) \approx 40W_1^{self}$, but this represents probably an overestimate, since the theory was constructed to deal with strongly polarizable ions. This limit is opposite to that treated by KU, applicable to hard nonpolarizable ions.

5. Concluding Remarks

In this work, we present a careful analysis of the electrostatic free energy of a finite-sized semipolarizable spherical ion, uniformly charged on its surface, crossing a sharp planar interface between two semi-infinite dielectric media. By considering the absence of dielectric contrast between the ion core and the external medium where it is embedded—as also implicitly assumed in prior works[58,59]—for the case without penetration, we obtain the classical point-charge result. Important deviations occur only when there is ionic penetration into the dielectric interface. However, the proper account of the image charges associated with the electrostatic problem shows that previous results[58,59] underestimate the electrostatic free energy for an ion modeled as a vacuum cavity at the interface by more than an order of magnitude.

The analysis also elucidates the role of the ionic polarizability: as already emphasized by Levin,[18,19] hard nonpolarizable ions (such as alkali metal cations, modeled as vacuum cavities) are associated with higher free energies than the soft highly polarizable ions (such as larger halogen anions, I^- and Br^-, modeled as conducting spheres). Since the electrostatic free energy of polarizable ions is so much lower than that of hard nonpolarizable ions, they might be adsorbed to the water−vapor interface as a result of cavitation.[18,19] This adsorption, verified in recent experiments and molecular-dynamics simulations,[46−50] is in clear contradiction to the classical WOS view.[44,45] According to the latter, ions should be repelled from hydrophobic surfaces due to image−charge repulsive interactions.

In our simplified model, the point-charge approximation, eqs 2 and 3, represents an exact result in the absence of penetration. When extended up to the penetration region, it leads to spurious singularities for a sharp planar dielectric interface. This anomaly does not occur in our model as a consequence of the finite ionic size. As already commented at the end of subsection 3.1, the above-mentioned effects, due to finite ionic size and polarizability, are thus usually negligible, unless the ion is very close to the interface. Even for an atomically neat interface, one might expect that at least one or two molecular layers apart, the solvent will behave differently from the bulk. Classical continuum dielectric theory, however, completely ignores the molecular nature of the interface. In this case, its strict use with a sharp step-like interface to describe its behavior might be questionable.

On the other hand, an alternative form to get rid of the above-mentioned singularities is to take into account a gradual change of the dielectric properties across the interface, but still considering point-like ions. Although a more accurate treatment of this effect should consider the dipolar nature of the aqueous solvent,[90,91] one might consider a phenomenological model within a continuum dielectric theory in which the transition layer of the implicit solvent is implemented in an effective way by the introduction of a continuous inhomogeneity of the dielectric profile across the GDS.[92−94] From the theoretical point of view, this procedure is justified within the framework of nonlocal electrostatics.[95] This assumption has been used, for example, to analyze atomic-force microscopy experimental measurements at liquid−gas and liquid−solid interfaces,[96,97] allowing local effective aqueous dielectric profiles to be obtained. In an analogous way, one may also take the interface roughness into account,[98] associated with fluctuations around the neat flat geometry. Both effects eliminate the divergence of the point-charge free energy at the GDS.[92−94,98] All of the previously mentioned aspects—finite size and polarizability of the ions, smoothness of the dielectric profile, and roughness of the dielectric interface—have been treated separately through different simplified models using an implicit solvent. In a real system, these features are not independent but correlated. It should be remarked, however, that the current approach,

focusing on the finite ionic size, is the simplest—though nontrivial—and the most physically transparent way to obtain a singularity-free estimate of the free energy associated with ionic transfer across a dielectric interface. It would be interesting to consider a model which incorporates all of these distinct effects, in order to estimate their relative contributions to the system free energy. However, in view of the complexity of the resulting problem, its investigation is beyond the scope of the present work.

Acknowledgment. This work is supported by FAPESP (Fundação de Amparo à Pesquisa do Estado de São Paulo). M.N.T. acknowledges fruitful discussions with Y. Levin and A.K.T. Assis.

A. Electrostatic Potential

In this Appendix, we give explicit expressions of the electrostatic potential Ψ of the system. In view of the spherical symmetry of the ionic free-charge distribution, $\rho(\mathbf{r}) = \sigma\delta(|\mathbf{r}| - a)$, with $\sigma = q/4\pi a^2$, and the assumption of the same dielectric constant of the ion core as of the external medium, it is straightforward to exactly solve the electrostatic problem by the image−charge method.[81−83] One needs to treat the cases without ($|h| \geq a$) and with penetration ($|h| < a$) separately.

A.1. Case without Penetration, $|h| \geq a$. For the case without penetration, when the ion—with internal dielectric constant ε_1—is completely immersed in region I, it is trivial to solve the electrostatic problem by applying the standard image−charge method.[81−83] In this case, the exact solution of the electrostatic problem reduces to point-charge expressions

$$\Psi_{1<} = \frac{q}{\varepsilon_1 a} + \frac{\lambda q}{\varepsilon_1 r'} \qquad \mathbf{E}_{1<} = \frac{\lambda q \hat{\mathbf{r}}'}{\varepsilon_1 r'^2} \tag{A.1}$$

$$\Psi_{1>} = \frac{q}{\varepsilon_1 r} + \frac{\lambda q}{\varepsilon_1 r'} \qquad \mathbf{E}_{1>} = \frac{q\hat{\mathbf{r}}}{\varepsilon_1 r^2} + \frac{\lambda q \hat{\mathbf{r}}'}{\varepsilon_1 r'^2} \tag{A.2}$$

$$\Psi_2 = \frac{q}{\varepsilon_2 r}(1 - \lambda) \qquad \mathbf{E}_2 = \frac{q\hat{\mathbf{r}}}{\varepsilon_2 r^2}(1 - \lambda) \tag{A.3}$$

in which $\mathbf{r} \equiv \mathbf{R} - h\hat{\mathbf{z}}$ and $\mathbf{r}' \equiv \mathbf{R} + h\hat{\mathbf{z}}$ are coordinates relative to the ion and image−charge centers and $\hat{\mathbf{r}} \equiv \mathbf{r}/r$ and $\hat{\mathbf{r}}' \equiv \mathbf{r}'/r'$ are the associated unit vectors—see Figure 1. The subscripts 1<, 1> and 2 label the regions inside ($Z > 0$, $r < a$) and outside ($Z > 0$, $r \geq a$) the ion in region I and region II ($Z < 0$), respectively.

In order to determine the electrostatic potential for the symmetric case when the ion has internal dielectric constant ε_2 and is entirely in region II ($h \leq -a$), we switch the dielectric constants $\varepsilon_1 \rightleftarrows \varepsilon_2$ and the labeling of the three distinct regions

$$\Psi_1 = \frac{q}{\varepsilon_1 r}(1 + \lambda) \qquad \mathbf{E}_1 = \frac{q\hat{\mathbf{r}}}{\varepsilon_1 r^2}(1 + \lambda) \tag{A.4}$$

$$\Psi_{2<} = \frac{q}{\varepsilon_2 a} - \frac{\lambda q}{\varepsilon_2 r'} \qquad \mathbf{E}_{2<} = -\frac{\lambda q \hat{\mathbf{r}}'}{\varepsilon_2 r'^2} \tag{A.5}$$

$$\Psi_{2>} = \frac{q}{\varepsilon_2 r} - \frac{\lambda q}{\varepsilon_2 r'} \qquad \mathbf{E}_{2>} = \frac{q\hat{\mathbf{r}}}{\varepsilon_2 r^2} - \frac{\lambda q \hat{\mathbf{r}}'}{\varepsilon_2 r'^2} \tag{A.6}$$

Now the subscripts 1, 2< and 2> label the regions I ($Z > 0$) and inside ($Z < 0$, $r < a$) and outside ($Z < 0$, $r \geq a$) the ion in region II, respectively.

In both cases, when the ion is entirely immersed in each of the two homogeneous media ($|h| \geq a$), the point-charge expressions of the electrostatic potential, eqs A.1−A.6, follow from the method of images, spherical symmetry of the ionic free-charge surface distribution, spherical symmetry of the image−charge distribution, and the assumption that there is no dielectric contrast between the ion core and the external dielectric medium where it is embedded. Since KU[58,59] also used these point-charge potentials, the latter condition of absence of dielectric contrast, though not clearly expressed in their papers, was implicit in their calculations. The existence of any dielectric contrast across the ionic surface would require a more sophisticated treatment of the electrostatic problem,[38,72,73] preventing a transparent and uncomplicated analysis, even for the simpler case in the absence of penetration.

A.2. Case with Penetration, $|h| < a$. For the case with partial ionic penetration into the dielectric interface, the condition of spherical symmetry of the charge distributions is not fulfilled, as sketched in Figure 2 and explained in section 3.2. Therefore, the point-charge expressions for Ψ, eqs A.1−A.6, can no longer be used in this case. Despite the lack of spherical symmetry of the charge distributions, which makes the problem more intricate, the image−charge method[81−83] may still be used to derive the electrostatic potential.

The electrostatic potential Ψ_k in region k may be obtained by the general solution of Poisson's equation boundary-value problem, expressed in terms of Green's function[83] for the bare electrostatic potential renormalized by the dielectric constant ε_k

$$\Psi_k(\mathbf{R}) = \int \frac{\rho_k(\mathbf{R}')\, \mathrm{d}^3\mathbf{R}'}{\varepsilon_k |\mathbf{R} - \mathbf{R}'|} \tag{A.7}$$

where ρ_k are the effective charge distributions for the determination of the electrostatic potential in regions I and II, which are depicted in Figure 2. They can be formally written as

$$\rho_1(\mathbf{R}) = [\sigma + (\sigma_B - \sigma)\Theta_{-1,-x}(\cos\theta)]\delta(r - a) + \sigma_A \Theta_{-1,x}(\cos\theta')\delta(r' - a) \tag{A.8}$$

$$\rho_2(\mathbf{R}) = [\sigma + (\sigma_D - \sigma)\Theta_{-x,1}(\cos\theta)]\delta(r - a) + \sigma_C \Theta_{x,1}(\cos\theta')\delta(r' - a) \tag{A.9}$$

$$\Theta_{\alpha\beta}(\gamma) \equiv \Theta(\gamma - \alpha)\Theta(\beta - \gamma) \tag{A.10}$$

where $\mathbf{r} \equiv \mathbf{R} - h\hat{\mathbf{z}}$, $\mathbf{r}' \equiv \mathbf{R} + h\hat{\mathbf{z}}$ are coordinates relative to the ionic center and its mirror image, $\theta = \arccos(\hat{\mathbf{r}}\cdot\hat{\mathbf{z}})$, $\theta' = \arccos(\hat{\mathbf{r}}'\cdot\hat{\mathbf{z}})$—see Figure 2—and $\Theta(x)$ is the usual Heaviside step function.

Since our final goal is to calculate the electrostatic free energy W by using eq 9, it is sufficient to obtain the electrostatic potential Ψ at the ionic charged surface $r = a$. After substituting eqs A.8 and A.9 into A.7 and performing the integrations over the azimuthal angle ϕ', we obtain

$$\Psi_1(r=a, 0 \le \theta \le \vartheta) = \frac{q}{\varepsilon_1 a} + \frac{4a\sigma_A}{\varepsilon_1\sqrt{2}} \int_{-1}^{x} \mathrm{d}(\cos\theta') \frac{K\left[\frac{2\sin\theta\sin\theta'}{1-\cos(\theta+\theta')+f_-(\theta,\theta',x)}\right]}{\sqrt{1-\cos(\theta+\theta')+f_-(\theta,\theta',x)}} + \frac{4a(\sigma_B-\sigma)}{\varepsilon_1\sqrt{2}} \int_{x}^{1} \mathrm{d}(\cos\theta') \frac{K\left[\frac{2\sin\theta\sin\theta'}{1+\cos(\theta-\theta')}\right]}{\sqrt{1+\cos(\theta-\theta')}} \quad \text{(A.11)}$$

$$\Psi_2(r=a, \vartheta \le \theta \le \pi) = \frac{q}{\varepsilon_2 a} + \frac{4a\sigma_C}{\varepsilon_2\sqrt{2}} \int_{-1}^{-x} \mathrm{d}(\cos\theta') \frac{K\left[\frac{2\sin\theta\sin\theta'}{1+\cos(\theta-\theta')+f_+(\theta,\theta',x)}\right]}{\sqrt{1+\cos(\theta-\theta')+f_+(\theta,\theta',x)}} + \frac{4a(\sigma_D-\sigma)}{\varepsilon_2\sqrt{2}} \int_{-x}^{1} \mathrm{d}(\cos\theta') \frac{K\left[\frac{2\sin\theta\sin\theta'}{1-\cos(\theta+\theta')}\right]}{\sqrt{1-\cos(\theta+\theta')}} \quad \text{(A.12)}$$

with $\vartheta = \arccos(-x)$, $f_\pm(\theta, \theta', x) = 2x(\cos\theta \pm \cos\theta' + x)$ and $K[m]$ is the complete elliptic integral of the first kind[88,89]

$$K[m] \equiv \int_0^{\pi/2} \frac{\mathrm{d}\alpha}{\sqrt{1-m\sin^2\alpha}} \quad \text{(A.13)}$$

B. Alternative Derivation of the Electrostatic Free Energy, Case without Penetration, $|h| \ge a$

In this Appendix, we show, by using different integration forms, that eqs 9 and 10 also lead to the classical point-charge electrostatic free energy, eq 2, when there is no ionic penetration.

The electrostatic free energy given by eq 9 is easily obtained considering the surface *free*-charge density $\rho(\mathbf{r}) = \sigma\delta(|\mathbf{r}| - a)$, with $\sigma = q/4\pi a^2$, and the electrostatic potential valid for $h \ge a$, eqs A.1 and A.2,

$$W(x \ge 1) = \frac{1}{2}\int_{r=a} \sigma\Psi_1 \,\mathrm{d}S_1 = \frac{q^2}{2\varepsilon_1 a}\left(1 + \frac{\lambda}{2x}\right) \quad \text{(B.1)}$$

with $\Psi_1 \equiv \Psi_{1>} = \Psi_{1<}$ along the spherical surface of integration at $r = a$ and the infinitesimal surface element $\mathrm{d}S_1 = a^2\mathrm{d}\phi\mathrm{d}(\cos\theta)$. This result, as expected, is in agreement with the classical point-charge result,[5] eq 2.

Finally, one could also obtain the electrostatic free energy $W = W_> + W_<$ by using the volumetric integral of $\mathbf{D}\cdot\mathbf{E}$ over the whole space, since in this case the surface terms of eq 10 at infinity vanish

$$W_> \equiv \frac{\varepsilon_1}{8\pi}\int_{V_{1>}} |\mathbf{E}_{1>}|^2 \,\mathrm{d}^3\mathbf{r} + \frac{\varepsilon_2}{8\pi}\int_{V_2} |\mathbf{E}_2|^2 \,\mathrm{d}^3\boldsymbol{r} \quad \text{(B.2)}$$

$$W_< \equiv \frac{\varepsilon_1}{8\pi}\int_{V_{1<}} |\mathbf{E}_{1<}|^2 \,\mathrm{d}^3\mathbf{r} \quad \text{(B.3)}$$

in which $V_{1>}$ and $V_{1<}$ are the volumes in region I outside ($Z > 0$, $r > a$) and inside the ion ($Z > 0$, $r < a$) and V_2 is the volume of region II ($Z < 0$). Using the electric fields given by eqs A.1−A.3, the above integrations coincide with eqs 11 and 12 and we are again led to the classical point-charge electrostatic free energy given by eq 2.

References and Notes

(1) Feynman, R. P.; Leighton, R. B.; Sands, M. *The Feynman Lectures on Physics, Mainly Electromagnetism and Matter*; Addison-Wesley: Reading, MA, 1964; Vol. 2, Chapter 9.
(2) Melehy, M. A. *Introduction to Interfacial Transport: A Generalization of Einstein's Theory of Brownian Motion with Interdisciplinary Applications*; AuthorHouse: Bloomington, IN, 2009.
(3) Fröhlich, H. *Theory of Dielectrics: Dielectric Constant and Dielectric Loss*, 2nd ed.; Clarendon Press: Oxford, U.K., 1958.
(4) Böttcher, C. J. F. *Theory of Electric Polarization*, 2nd ed.; Elsevier: Amsterdam, The Netherlands, 1973; Vol. I (Dielectrics in static fields).
(5) Landau, L. D.; Lifshitz, E. M. *Electrodynamics of Continuous Media*, 2nd ed.; Pergamon: Oxford, U.K., 1984.
(6) Kirkwood, J. G. *J. Chem. Phys.* **1934**, *2*, 351. Erratum: **1934**, *2*, 713.
(7) Tanford, C.; Kirkwood, J. G. *J. Am. Chem. Soc.* **1957**, *79*, 5333.
(8) Conway, B. E. *Ionic Hydration in Chemistry and Biophysics*; Elsevier: Amsterdam, The Netherlands, 1981.
(9) Honig, B.; Nicholls, A. *Science* **1995**, *268*, 1144.
(10) Levin, Y. *J. Chem. Phys.* **2008**, *129*, 124712.
(11) Onuki, A. *Phys. Rev. E* **2006**, *73*, 021506; *Europhys. Lett.* **2008**, *82*, 58002; *J. Chem. Phys.* **2008**, *128*, 224704.
(12) de Graaf, J.; Zwanikken, J.; Bier, M.; Baarsma, A.; Oloumi, Y.; Spelt, M.; van Roij, R. *J. Chem. Phys.* **2008**, *129*, 194701.
(13) Zwanikken, J.; de Graaf, J.; Bier, M.; van Roij, R. *J. Phys.: Condens. Matter* **2008**, *20*, 494238.
(14) Bier, M.; Zwanikken, J.; van Roij, R. *Phys. Rev. Lett.* **2008**, *101*, 046104.
(15) Levin, Y. *J. Chem. Phys.* **2000**, *113*, 9722.
(16) Levin, Y.; Flores-Mena, J. E. *Europhys. Lett.* **2001**, *56*, 187.
(17) Pegram, L. M.; Record, M. T., Jr. *Proc. Natl. Acad. Sci. U.S.A.* **2006**, *103*, 14278.
(18) Levin, Y. *Phys. Rev. Lett.* **2009**, *102*, 147803.
(19) Levin, Y.; dos Santos, A. P.; Diehl, A. *Phys. Rev. Lett.* **2009**, *103*, 257802.
(20) Marcus, R. A. *J. Phys. Chem.* **1990**, *94*, 1050.
(21) Benjamin, I. *Science* **1993**, *261*, 1558.
(22) Parsegian, A. *Nature* **1969**, *221*, 844.
(23) Benjamin, I. *Chem. Rev.* **1996**, *96*, 1449.
(24) Wu, K.; Iedema, M. J.; Cowin, J. P. *Science* **1999**, *286*, 2482.
(25) Jungwirth, P.; Tobias, D. J. *Chem. Rev.* **2006**, *106*, 1259.
(26) Chang, T. M.; Dang, L. X. *Chem. Rev.* **2006**, *106*, 1305.
(27) Luo, G.; Malkova, S.; Yoon, J.; Schultz, D. G.; Lin, B.; Meron, M.; Benjamin, I.; Vanýsek, P.; Schlossman, M. L. *Science* **2006**, *311*, 216.
(28) Kung, W.; Solis, F. J.; de la Cruz, M. O. *J. Chem. Phys.* **2009**, *130*, 044502.
(29) Rao, Y.; Subir, M.; McArthur, E. A.; Turro, N. J.; Eisenthal, K. B. *Chem. Phys. Lett.* **2009**, *477*, 241.
(30) Mundy, C. J.; Kuo, I.-F. W.; Tuckerman, M. E.; Lee, H.-S.; Tobias, D. *J. Chem. Phys. Lett.* **2009**, *481*, 2.
(31) Tian, C. S.; Shen, Y. R. *Proc. Natl. Acad. Sci. U.S.A.* **2009**, *106*, 15148.
(32) Craig, V. S. J.; Ninham, B. W.; Pashley, R. M. *Nature* **1993**, *364*, 317.
(33) Flatté, M. E.; Kornyshev, A. A.; Urbakh, M. *Proc. Natl. Acad. Sci. U.S.A.* **2008**, *105*, 18212.
(34) Seinfeld, J. H. *Science* **2000**, *288*, 285.
(35) Knipping, E. M.; Lakin, M. J.; Foster, K. L.; Jungwirth, P.; Tobias, D. J.; Gerber, R. B.; Dabdub, D.; Finlayson-Pitts, B. J. *Science* **2000**, *288*, 301.
(36) O'Dowd, C. D.; Jimenez, J. L.; Bahreini, R.; Flagan, R. C.; Seinfeld, J. H.; Hämeri, K.; Pirjola, L.; Kulmala, M.; Jennings, S. G.; Hoffmann, T. *Nature* **2002**, *417*, 632.
(37) Shannon, M. A.; Bohn, P. W.; Elimelech, M.; Georgiadis, J. G.; Mariñas, B. J.; Mayes, A. M. *Nature* **2008**, *452*, 301.
(38) Danov, K. D.; Kralchevsky, P. A.; Ananthapadmanabhan, K. P.; Lips, A. *Langmuir* **2006**, *22*, 106.
(39) Zwanikken, J.; van Roij, R. *Phys. Rev. Lett.* **2007**, *99*, 178301.
(40) Leunissen, M. E.; van Blaaderen, A.; Hollingsworth, A. D.; Sullivan, M. T.; Chaikin, P. M. *Proc. Natl. Acad. Sci. U.S.A.* **2007**, *104*, 2585.
(41) Leunissen, M. E.; Zwanikken, J.; van Roij, R.; Chaikin, P. M.; van Blaaderen, A. *Phys. Chem. Chem. Phys.* **2007**, *9*, 6405.
(42) Hatlo, M. M.; Lue, L. *Soft Matter* **2008**, *4*, 1582.
(43) Heydweiller, A. *Ann. Phys. (Leipzig)* **1910**, *33*, 145.
(44) Wagner, C. *Phys. Z.* **1924**, *25*, 474.
(45) Onsager, L.; Samaras, N. N. T. *J. Chem. Phys.* **1934**, *2*, 528.
(46) Jungwirth, P.; Tobias, D. J. *J. Phys. Chem. B* **2002**, *106*, 6361.
(47) Garrett, B. C. *Science* **2004**, *303*, 1146.

(48) Ghosal, S.; Hemminger, J. C.; Bluhm, H.; Mun, B. S.; Hebenstreit, E. L. D.; Ketteler, G.; Ogletree, D. F.; Requejo, F. G.; Salmeron, M. *Science* **2005**, *307*, 563.
(49) Horinek, D.; Herz, A.; Vrbka, L.; Sedlmeier, F.; Mamatkulov, S. I.; Netz, R. R. *Chem. Phys. Lett.* **2009**, *479*, 173.
(50) Noah-Vanhoucke, J.; Geissler, P. L. *Proc. Natl. Acad. Sci. U.S.A.* **2009**, *106*, 15125.
(51) Frumkin, A. *Z. Phys. Chem.* **1924**, *109*, 34.
(52) Hofmeister, F. *Arch. Exp. Pathol. Pharmakol.* **1888**, *24*, 247.
(53) Collins, K. D.; Washabaugh, M. W. *Q. Rev. Biophys.* **1985**, *18*, 323.
(54) Parsegian, V. A. *Nature* **1995**, *378*, 335.
(55) Cacace, M. G.; Landau, E. M.; Ramsden, J. J. *Q. Rev. Biophys.* **1997**, *30*, 241.
(56) Kunz, W.; Lo Nostro, P.; Ninham, B. W. *Curr. Opin. Colloid Interface Sci.* **2004**, *9*, 1.
(57) Zhang, Y.; Cremer, P. S. *Curr. Opin. Chem. Biol.* **2006**, *10*, 658.
(58) Kharkats, Yu. I.; Ulstrup, J. *J. Electroanal. Chem.* **1991**, *308*, 17.
(59) Ulstrup, J.; Kharkats, Yu. I. *Élektrokhimiya* **1993**, *29*, 299. Engl. Transl. in *Russ. J. Electrochem.* **1993**, *29*, 386.
(60) Born, M. *Z. Phys.* **1920**, *1*, 45.
(61) Volkov, A. G.; Deamer, D. W.; Tanelian, D. L.; Markin, V. S. *Prog. Surf. Sci.* **1996**, *53*, 1.
(62) Benjamin, I. *Annu. Rev. Phys. Chem.* **1997**, *48*, 407.
(63) Tamburello-Luca, A. A.; Hébert, P.; Antoine, R.; Brevet, P. F.; Girault, H. H. *Langmuir* **1997**, *13*, 4428.
(64) Wu, K.; Iedema, M. J.; Schenter, G. K.; Cowin, J. P. *J. Phys. Chem. B* **2001**, *105*, 2483.
(65) Johnson, A.-C. J. H.; Greenwood, P.; Hagström, M.; Abbas, Z.; Wall, S. *Langmuir* **2008**, *24*, 12798.
(66) Tikhonov, A. M. *J. Chem. Phys.* **2009**, *130*, 024512.
(67) Horinek, D.; Netz, R. R. *Phys. Rev. Lett.* **2007**, *99*, 226104.
(68) Horinek, D.; Serr, A.; Bonthuis, D. J.; Boström, M.; Kunz, W.; Netz, R. R. *Langmuir* **2008**, *24*, 1271.
(69) Markin, V. S.; Volkov, A. G. *J. Phys. Chem. B* **2002**, *106*, 11810.
(70) Boström, M.; Ninham, B. W. *Langmuir* **2004**, *20*, 7569.
(71) van der Zwan, G.; Mazo, R. M. *J. Chem. Phys.* **1985**, *82*, 3344.
(72) Buff, F. P.; Goel, N. S. *J. Chem. Phys.* **1972**, *56*, 2405.
(73) Buff, F. P.; Goel, N. S.; Clay, J. R. *J. Chem. Phys.* **1975**, *63*, 1367.
(74) Linse, P. *J. Phys. Chem.* **1986**, *90*, 6821.
(75) Iversen, G.; Kharkats, Yu. I.; Ulstrup, J. *Mol. Phys.* **1998**, *94*, 297.
(76) Messina, R. *J. Chem. Phys.* **2002**, *117*, 11062.
(77) Tamashiro, M. N.; Schiessel, H. *Phys. Rev. E* **2006**, *74*, 021412.
(78) Linse, P. *J. Chem. Phys.* **2008**, *128*, 214505.
(79) Gibbs, J. W. *The Collected Works of J. W. Gibbs*; Longmans: New York, 1928; Vol. I (Thermodynamics), p. 219.
(80) Levin, Y. *J. Stat. Phys.* **2003**, *110*, 825.
(81) Maxwell, J. C. *A Treatise on Electricity and Magnetism*, unabridged 3rd ed.; Dover: New York, 1954; Vol. 1, Chapter XI.
(82) Smythe, W. R. *Static and Dynamic Electricity*, 3rd ed.; McGraw-Hill: New York, 1968.
(83) Jackson, J. D. *Classical Electrodynamics*, 3rd ed.; John Wiley & Sons: Berkeley, CA, 1999.
(84) It should be remarked that a uniform and spherically symmetric ionic *volumetric* charge density $\rho(\mathbf{r}) = 3q/4\pi a^3$, $0 \leq |\mathbf{r}| \leq a$, distributed within a dielectric sphere of internal dielectric constant ε^{in} immersed in a bulk medium of dielectric constant ε^{out} leads to an ionic self-energy $W^{self} = (q^2/2a)[(\varepsilon^{out})^{-1} + (5\varepsilon^{in})^{-1}]$, instead of $W^{self} = q^2/2\varepsilon^{out}a$ obtained for a uniform *surface* charge distribution. Since later we want to compare our results with the existing KU calculations,[47,48] this justifies the choice of the ionic charge distributed uniformly onto its surface.
(85) Debye, P.; Hückel, E. *Phys. Z.* **1923**, *24*, 185, 305.
(86) McQuarrie, D. A. *Statistical Mechanics*; University Science Books: Sausalito, CA, 2000; Chapter 15.
(87) Güntelberg, E. *Z. Phys. Chem.* **1926**, *123*, 199.
(88) Abramowitz, M.; Stegun, I. A. *Handbook of Mathematical Functions with Formulas, Graphs, and Mathematical Tables*, 10th printing; U.S. Government Printing Office: Washington D.C., 1972.
(89) Gradshteyn, I. S.; Ryzhik, I. M. (edited by Jeffrey, A.; Zwillinger, D.). *Table of Integrals, Series, and Products*, 7th ed.; Elsevier Academic Press: Burlington, MA, 2007.
(90) Finken, R.; Ballenegger, V.; Hansen, J.-P. *Mol. Phys.* **2003**, *101*, 2559.
(91) Ballenegger, V.; Hansen, J.-P. *Europhys. Lett.* **2003**, *63*, 381; *J. Chem. Phys.* **2005**, *122*, 114711.
(92) Buff, F. P.; Goel, N. S. *J. Chem. Phys.* **1969**, *51*, 4983, 5363.
(93) Stern, F. *Phys. Rev. B* **1978**, *17*, 5009.
(94) Nakamura, T. *J. Phys. Soc. Jpn.* **1983**, *52*, 973.
(95) Hildebrandt, A.; Blossey, R.; Rjasanow, S.; Kohlbacher, O.; Lenhof, H.-P. *Phys. Rev. Lett.* **2004**, *93*, 108104.
(96) Teschke, O.; Ceotto, G.; de Souza, E. F. *Chem. Phys. Lett.* **2000**, *326*, 328; *Phys. Chem. Chem. Phys.* **2001**, *3*, 3761; *Phys. Rev. E* **2001**, *64*, 011605.
(97) Teschke, O.; de Souza, E. F. *Langmuir* **2003**, *19*, 5357; *Chem. Phys. Lett.* **2005**, *403*, 95.
(98) Rahman, T. S.; Maradudin, A. A. *Phys. Rev. B* **1980**, *21*, 504.

JP911898T